2 EXPERIMENTAL FACILITIES

2.1 The Seitz shock tube

2.1.1 Background

A shock tube is used to generate a moving shock wave with predetermined strength. A region of constant pressure, temperature and gas velocity is generated behind the incident plane shock front. The simplest shock tube has a constant cross-section and comprises of a compression chamber, a bursting disc or diaphragm, and an expansion chamber.

When the compression chamber is filled with gas to a specified pressure the diaphragm ruptures leading to the generation of a plane moving shock wave. A region of constant pressure and velocity is established behind the advancing shock wave. A contact surface separates the expansion chamber gas from the escaping compression chamber gas. An expansion fan then moves back into the compression chamber and reflects off the back wall.

To achieve higher Mach numbers at the same compression chamber pressure one can use multiple diaphragms. The compression wave resulting from the normal bursting of a first diaphragm heats and pressurises the gas in an intermediate compression chamber, prior to the bursting of a second diaphragm. The bursting of the second diaphragm then occurs either by an external mechanical means or by over-pressurisation.

2.1.2 The shock tube facility

The ‘Seitz’ shock tube in the School of Mechanical Engineering at the University of the Witwatersrand will be used for the author’s research. The shock tube was used to generate a planar shock wave that would pass over several test pieces in order to investigate the resulting reflected wave structures. The design and manufacture of the shock tube facility was customized specially for automatic operation. A photograph of the facility can be seen in figure 2.1. The shock tube consists of a driver section (compression and intermediate chambers), expansion chamber, test section, support structure, and instrumentation for static and dynamic pressure measurement. A double self-rupturing diaphragm system is used to produce incident wave Mach

numbers ranging from 1.25 to 7. An optical system for flow visualisation is included in the test facility. The automation of the shock tube is controlled by a computer control system.

Figure 2.1: Shock tube facility at the University of the Witwatersrand.

The driver section

The driver section consists of the compression chamber and the intermediate chamber and has a safe operating pressure of 20 bar. The driver section has a length of 2 m and an internal diameter of 300 mm. The structural design was based on the standard steel pressure vessel design code BS5000 (Seitz 2001). The diaphragm configuration of the driver section is a double diaphragm arrangement, with a two-stage contraction geometry. The diaphragms are clamped between the flanges of the driver section by the use of a single hydraulic actuator. The piston and shaft of the actuator are held stationary while the compressive and intermediate chambers move on two straddling tie rods. The first contraction, located prior to the first diaphragm, transforms the circular cross-section of the compression chamber into a square cross-section (180 mm x 180 mm). The second contraction, located in the intermediate chamber, transforms the square cross-section to the rectangular cross-section of the expansion chamber (180 mm x 76 mm). Figure 2.2 illustrates shock tube cross section.

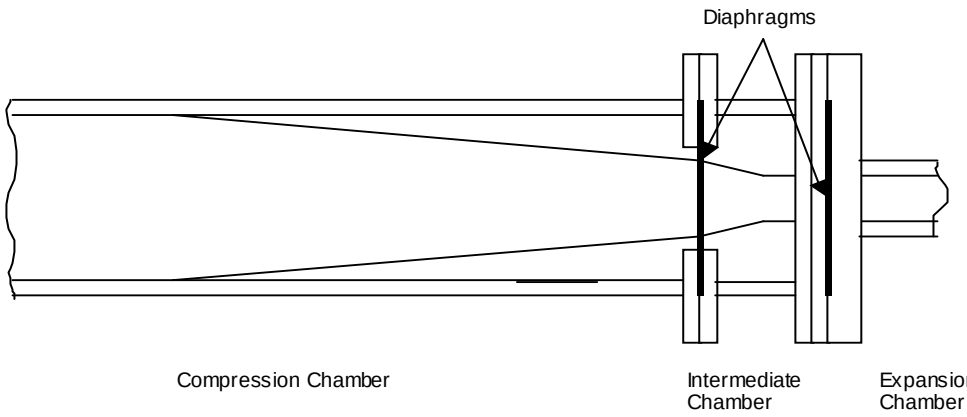

Figure 2.2: Cross-section of the shock tube illustrating contraction geometry and diaphragms.

The clamping of the diaphragm material between the flanges of the driver section is accomplished using a single hydraulic actuator mounted axially behind the compression chamber. In this arrangement, the piston and shaft of the actuator are held stationary while the compression chamber and intermediate chamber move on two straddling tie rods. Using this arrangement, the clamping force is applied while the hydraulic ram is extending. When the compression chamber is opened, the first and second diaphragm stations are opened automatically. To burst the diaphragms at a predetermined pressure, a method using the double-diaphragm arrangement is implemented. The intermediate and compression chambers are pressurised simultaneously, with the final pressure of the intermediate chamber being lower than that of the compression chamber. Once final pressurisation has been achieved the intermediate chamber is vented to the atmosphere, which results in an over-pressurisation causing the first diaphragm to burst. The second diaphragm, down stream, then bursts spontaneously due to the pressure behind the compression wave of the first burst diaphragm. Due to bulging and incomplete bursting of the polyester diaphragms, weak transverse waves originating from the diaphragm are often observed in the down stream flow field behind the incident shock wave. A 300 mm length thick-pile carpeting is permanently fixed against the top and bottom walls at the start of the expansion chamber to soothe these unwanted waves. Figure 2.3 illustrates all relevant driver section components.

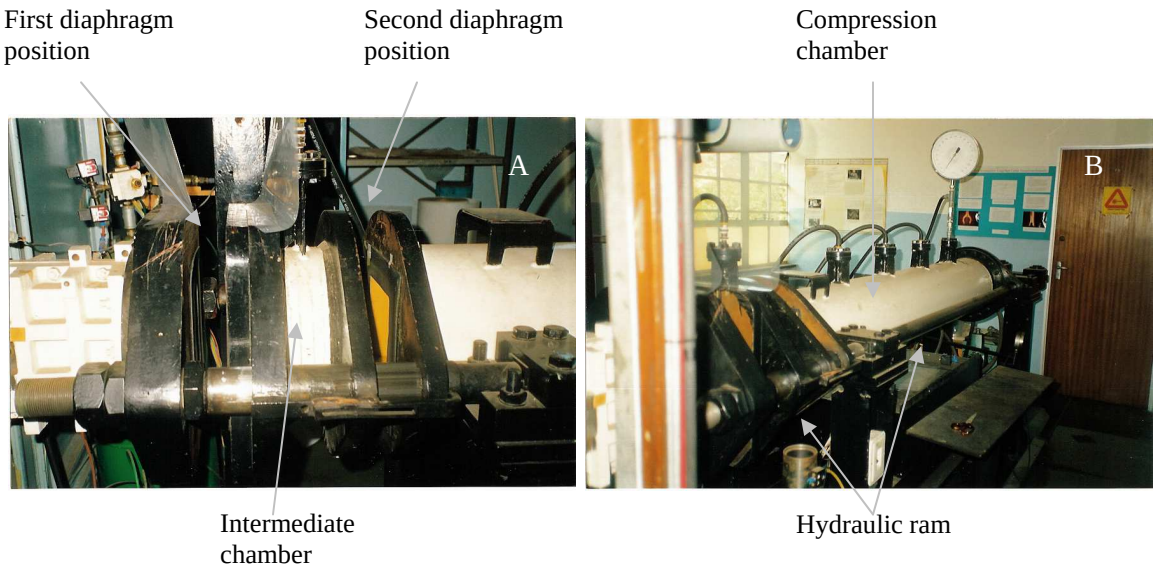

Figure 2.3: Photographs of driver section of the shock tube.

The expansion chamber

The expansion chamber (figure 2.4) of the shock tube has a length of 6 m with a 450 mm (internal) long test section situated at the end. The internal cross section of the expansion chamber is 180 mm x 76 mm. It is manufactured from cast iron, which allows reduction in wall vibrations due to it's superior damping properties. The expansion chamber is designed to operate at vacuum pressures down to 2 torr (Seitz 2001). Several ports along the expansion chamber, situated 450 mm apart, are available for pressure transducer installation. Two of these ports, closest to the test section, are fitted with pressure transducers used for calculating the actual Mach numbers of the tests and for initiating the recordings of the transducers in the test section.

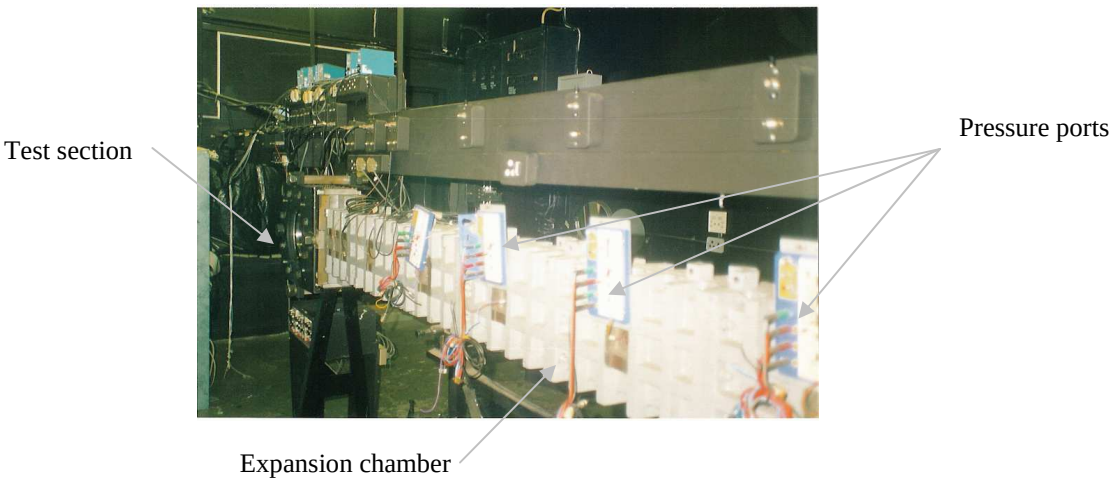

Figure 2.4: Photograph of expansion chamber of the shock tube.

The test section

The test section is located 6 m from the diaphragm station and is a smooth continuation of the expansion chamber. The top and bottom walls of the test section have transducer ports positioned at 30mm intervals along the centre-line along the length of the test section. All transducers (or brass blanks) are seated flush with the inner surface of the test section to prevent flow perturbations. The back wall also has ports for three transducers or one can make use of a back plate that increases the back wall transducer number to eight.

Both sides of the test section consist of hinged aluminium doors that incorporate optical glass windows, with spring plate support, for flow visualisation. The opening and closing of the test section simply involves loosening three large nuts on the doors and swinging their studs with the respective nuts clear of the spring plate. The door is then free to be opened on its hinges. The test section windows are manufactured from borosilicate crown optical quality glass and are circular in shape, having a view-filled diameter of 300 mm. The total viewing area of the test section is 180 mm x 180 mm. Figure 2.5 is a photograph of the test section.

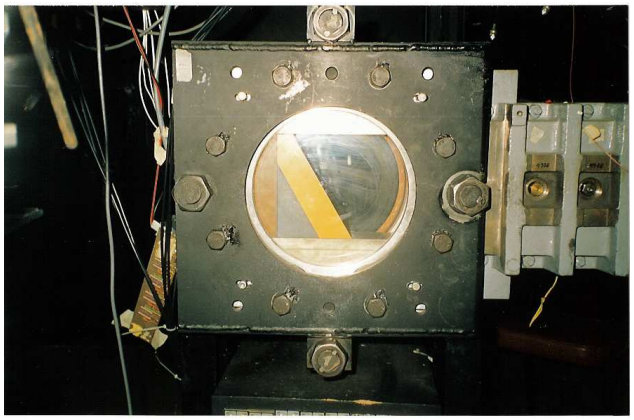

Figure 2.5: Photograph of test section of the shock tube.

Diaphragms

The incident shock strength is set by entering the desired Mach number into the computer control system. The software will then calculate the pressures required in each of the driven sections and according to the calibration tables, will determine the diaphragm thickness required. It outputs a thickness for diaphragm A and B, where A refers to the diaphragm that is inserted between the intermediate and expansion chambers and B refers to the diaphragm between the compression and intermediate chambers. The diaphragm material used is Polyester film.

Shock tube control system

The shock tube is fully automated by a computer control system. It consists of a desktop computer, an analogue to digital conversion system, and electro-pneumatic control system. The shock tube may also be manually operated through a series of valves and electrical switches. All processes are displayed on a computer monitor, including setup, operation and post-test data analysis.

The desktop computer software, “Shock”, has procedures for the pre-experiment setup of the system, for the operation of the tube and visualisation systems during the test run, and for any post-experiment data processing.

The pre-test-run functions allow for the calibration of the shock tube pressure system, ensuring that the pressure transducers are providing accurate feedback, and calibration of the flow visualisation system, ensuring a good optical setup before the test run begins.

During the test run the system closes the tube, pressurises the compression and intermediate chambers to the correct preset pressures, monitors for any premature diaphragm bursting, starts data capture from the instant of diaphragm rupture, opens the camera shutter, and strobes the xenon lamps at a specified time delay. The system can record up to eight pressure transducer traces.

2.2 Data acquisition system and instrumentation

2.2.1 Data acquisition system

The data acquisition system is situated in the expansion chamber room and consists of a personal computer and two A to D converters (ADC). Two 12 bit, 167 kHz, eight port Analogue to Digital converters are used to receive and store outputs from all measuring devices. Screened cables are used to transfer signals from the measuring devices to the ADC. The ADC used is a Rene Mauer ADAM (Analogue Data Acquisition Memory) with eight separate channels. Every channel uses input buffers to store digital data captured from the transducers. The digitised signals received are accessed from the personal computer. Software is used to convert the voltage signals from the transducers to pressure data. The data acquisition system can be seen in figure 2.6.

Figure 2.6: Photograph of the data acquisition system of the shock tube

2.2.2 Pressure and temperature measurements

Static pressure and temperature measurement

To allow the system to be optimised before each test run, ambient temperature and barometric pressure are required by the computer control system. Ambient temperature measurements are

achieved through integrated temperature sensors with accuracy of 0.25 °C (Seitz 2001) mounted above the test section. Barometric pressure is measured using a pressure transducer installed in the shock tube laboratory. The transducer has a resolution of 0.4mbar and factory set for a range of 800 –1 000 mbar.

Driver section pressure measurement

A high-pressure transducer with a measuring range of 0-20 bar gauge measures the pressure in the compression chamber and intermediate chamber. This transducer is designed to withstand any rapid pressure changes such as those caused by a diaphragm burst.

High-speed pressure measurement

All the pressure measurements inside the shock tube are measured using fast response PCB piezo-electric pressure transducers. The signals from these transducers are amplified by PCB line power units and received by the ADC.

2.3 Operation of the shock tube

The operation of the shock tube driver is entirely software controlled. The intermediate and compression chambers close when the automatic starting of the hydraulic pump is initiated, and subsequent actuation of an electrical solenoid valve controlling hydraulic oil flow. The hydraulic ram slowly moves the chambers to the closed position, clamping the diaphragms. The intermediate and compression chambers are then pressurised simultaneously to avoid overloading the diaphragm. The compression chamber is then further pressurised. The final pressure in the intermediate chamber is lower than in the compression chamber. The intermediate chamber is then vented increasing the pressure difference between it and the compression chamber thus causing the diaphragm to burst. This sends a shock wave down the expansion chamber. Once the shock wave has impacted with the back wall of the test section, the shock tube is then vented to atmosphere. When the pressure in the shock tube has reached atmospheric pressure, the chambers are opened. Diaphragm fragments are then removed from the shock tube after every test by blowing compressed air down the expansion and compression chambers.

2.4 The optical system

2.4.1 Distinction between Shadowgraph and Schlieren methods

Schlieren[3] and shadowgraph methods are closely related, but there are several distinctions. First, the shadowgram is not a focused optical image; it is a mere shadow. The schlieren image, however, is what it claims to be: an optical image formed by a lens, and thus bearing a conjugate optical relationship to the schlieren object. Second, schlieren methods require a knife-edge or some other cut-off of the refracted light, where no such cut-off is needed or allowed in shadowgraphy. Finally, the luminance level of a schlieren image responds to the first spatial derivative of the refracted index in the schlieren. The shadowgram, however, responds to the second spatial derivative or Laplacian. Equivalently, the schlieren image displays the deflection angle ε while shadowgraphy displays the ray displacement resulting from the deflection. Despite these distinctions, both schlieren and shadowgraphy are integrating optical systems that project line-of-sight information onto a viewing screen or camera focal plane.

Shadowgraphy allows large-scale visualisations and shows the salient features of a subject without gross change in illumination. Though it is less sensitive than schlieren in general, particular circumstances can make it more sensitive. Shadowgraphy renders, by way of its double differentiation, fine-scale images of turbulent flows. Shock waves, being natural step-functions, produce strong higher derivatives of refractive index that cause then to stand out as stark lines in a shadowgram. For weaker disturbances overall, however, schlieren holds the advantage of much higher sensitivity. Its unambiguous 1:1 image correspondence with the object of study is often a decisive benefit. It emphasises detail in the schlieren object where shadowgraphy usually downplays it. Thus many fields of application are open to the superior sensitivity and adaptability of the schlieren method that are closed to the simpler shadowgraph technique.

2.4.2 Shadowgraph technique

The shadowgraph technique is suitable for strong gradients creating sharp changes in screen illumination but not for mild gradients or quantitative evaluation. The great advantage of

[3] Schlieren are relatively small refractive differences that cause gradient disturbances of inhomogeneous transparent media. By definition they bend light rays in any other direction than the normal direction.

shadowgraphy is its extreme simplicity. Shadowgraph set-ups are quick and simple. It is adaptable to large fields-of-view. The optical quality requirements commonly consist of single-element lenses, Fresnel lenses and inexpensive mirrors. Shadowgrams may be cast on photographic film, on ground glass or projection screens, or on any reasonably flat, diffusely reflecting surface. In general, shadowgrams are not true to scale. Only the dark regions of a shadowgram can yield an undistorted representation of the schlieren object, since they mark where the deflected rays originate. The bright zones mark where these rays end up. Similarly, objects of significant extent along the optical axis in diverging light shadowgraphy suffer different magnifications of their near and far features in the shadowgram. An inversion of normal perspective occurs, in that the nearer an object is to the film plane, the smaller is its magnification. The resulting shape distortion is a problem if angular measurement is needed. It is however recommended the light source lie on a line through the model apex and perpendicular to the film plane in order to minimise this error.

2.4.3 Schlieren technique

To understand the basis of schlieren imaging, it helps to begin as simply as possibly with two lenses, geometric optics and a point light source. In a simple schlieren system with a point light source, a lens collimates the beam from the point source. A second lens refocuses the beam to an image of the point source. The beam then proceeds to a viewing screen where a real inverted image of the test area is formed. At this point the optical system is merely a projector, imaging opaque objects in the test area as silhouettes on the screen. Transparent schlieren objects are not imaged at all until a knife-edge is added at the focus of the second lens. As the knife-edge advances toward the focal point, nothing happens until it rather suddenly blocks the image of the light source, causing the screen to go dark. Thus one has the choice of a bright field or dark field. The orientation of the knife-edge determines what gradient components of the schlieren image are detected. The knife-edge affects only those ray refractions with components perpendicular to it. The Z-type 2-mirror schlieren system, shown in figure 2.7, is by far the most popular arrangement. Though tilted, the mirrors are usually symmetrical, on-axis parabolas. The advantage of parallel light equally applies to the Z-type mirror schlieren system.

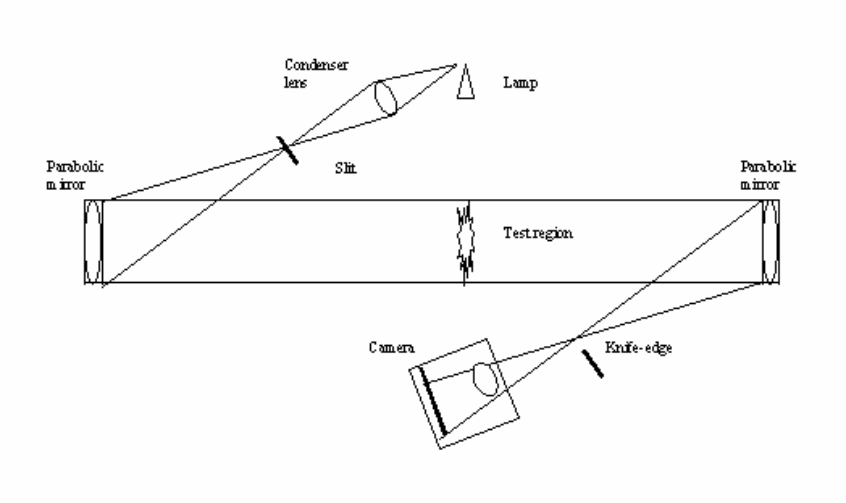

Figure 2.7: Z-type schlieren arrangement

2.4.4 The experimental optical system

The optical system for flow visualisation was initially set up to produce schlieren images. The system is based on the Z-type schlieren arrangement. A white light source, produced by a Xenon flash lamp, is passed through a thin slit, and then made parallel by using two parabolic mirrors. The Xenon flash lamp is mounted in adjustable holders that attach to, and slide on, steel rods situated on the light source column as seen in figure 2.8A. The two parabolic mirrors are 254mm in diameter and are mounted in fully adjustable mirror cells. Adjustable screws and bearings are located in the single support post. The mirror cells are mounted on heavy-base column support similar to those used for the light source system as seen in figure 2.8B. The parallel light is passed through the flow (in the test section) and then brought to a focus. The camera is arranged so that the test section of the shock tube is in focus. A knife-edge placed at the focal point is positioned so that it blocks roughly half of the light. The knife-edge, focussing lens and camera are integrated into a single fully adjustable unit as seen in figure 2.8C. If the flow is uniform, then the image behind the knife-edge will be uniformly bright. If the flow has refractive index variations that cause some of the light that would have passed by the knife-edge to instead be block by it, then the image has a dark area. Conversely, if the flow causes some light rays to pass the knife-edge that would otherwise have been blocked, then the image has light areas.

The optical system outlined above was easily adapted to produce shadowgraph images of the rectangular valley test pieces. The knife-edge was simply removed and a larger camera placed

before the second parabolic mirror as close to the test section window as possible. Precaution was taken to ensure that the camera was perpendicular to the window.

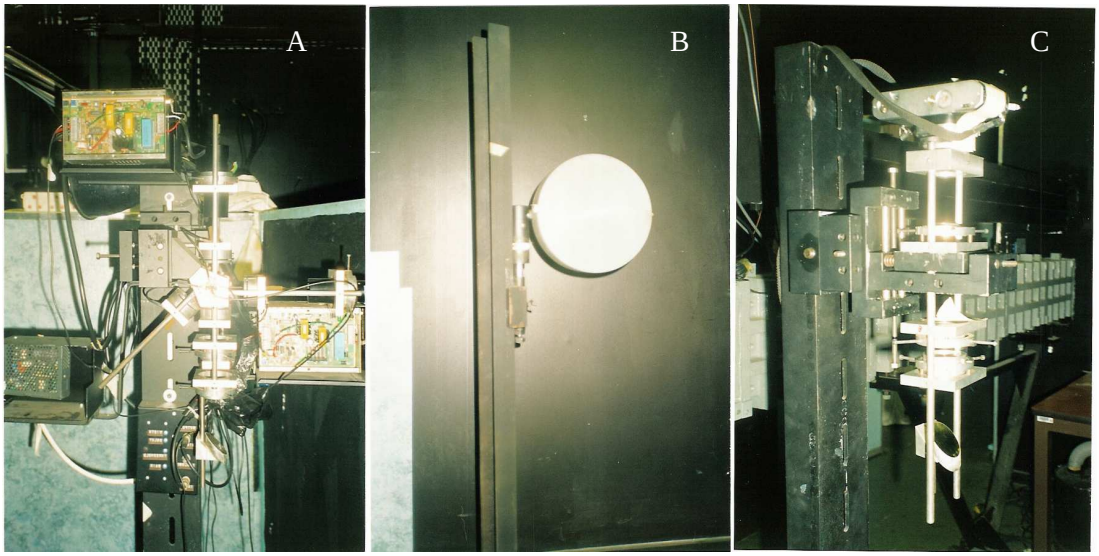

Figure 2.8: Photographs of the schlieren optical system.

2.5 The test pieces

2.5.1 Test pieces requirements

The aims of the research are to simulate the process of a supersonic aircraft entering a valley within a shock tube and determine the resulting three-dimensional wave structures. Figure 2.9 represents a schematic of an aircraft travelling at supersonic speeds close to the ground. One can see the generation of the bow wave. If the aircraft enters a valley, the three-dimensional bow wave reflected off the valley walls could focus behind the aircraft. If one rotates the physical geometry of an aircraft entering a valley at supersonic speeds, the bow wave can approximately be represented by a planar shock wave incident on a geometric valley structure. This structure can be represented by cutting a relevant valley shape into a wedge at a defined angle of inclination.

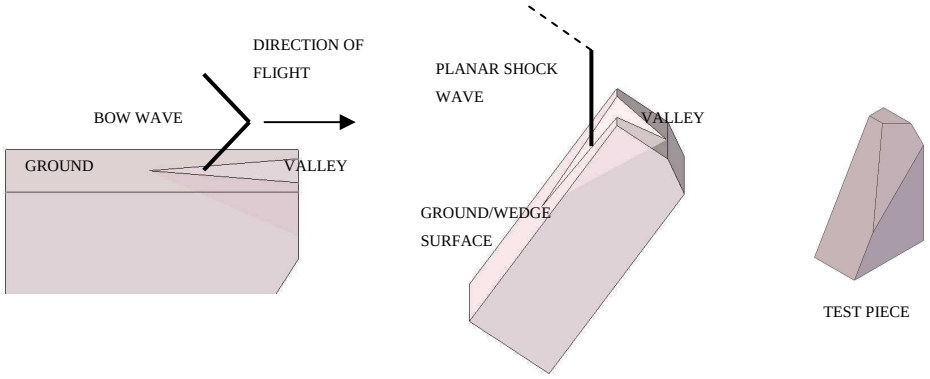

Figure 2.9: Schematic representation of a supersonic aircraft entering a valley

Experimentally, the shock wave structure can be examined by moving a planar shock wave, generated in a shock tube, over the before mentioned geometric structure. Due to the symmetry of the geometric structure only half of the valley need be represented. Shadowgraph and/or schlieren images can then be obtained to determine the resulting wave structures, and finally identifying a high pressure region arising from the focussing of the shock.

2.5.2 Test pieces

The four valley geometries under investigation are rectangular, triangular, parabolic and conical. The three hill geometries under investigation are triangular, parabolic and conical.

The various test pieces were manufactured from grey PVC. The wedges were cut at 60- and 70-degree inclinations (θ_w), ensuring regular reflection off the wedge surface (refer to appendix B for validation). The wedges have a height of 179mm and a base of 130mm. All valley/hill entrances were located on the wedge at a perpendicular height of 60mm from the base of wedge to ensure consistency.

The floor of the valley was set at four different inclinations for the rectangular and triangular valleys, namely 0, 15, 30 and 45 degrees relative to the base (θ_v). The rectangular valleys have a width of 37.5mm, exactly half the width of the wedge. The triangular wedges are cut with a 45-degree angle to the vertical axis at the back wall. Figures 2.10 and 2.11 illustrate the different rectangular and triangular valley geometries.

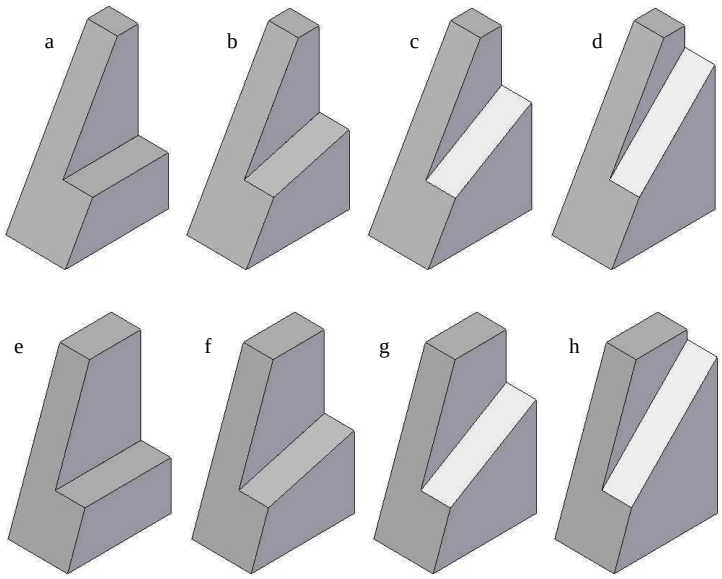

Figure 2.10: Rectangular valley test pieces

a) $\theta_w = 60^o$, $\theta_v = 0^o$ b) $\theta_w = 60^o$, $\theta_v = 15^o$ c) $\theta_w = 60^o$, $\theta_v = 30^o$ d) $\theta_w = 60^o$, $\theta_v = 45^o$

e) $\theta_w = 60^o$, $\theta_v = 0^o$ f) $\theta_w = 60^o$, $\theta_v = 15^o$ g) $\theta_w = 60^o$, $\theta_v = 30^o$ h) $\theta_w = 60^o$, $\theta_v = 45^o$

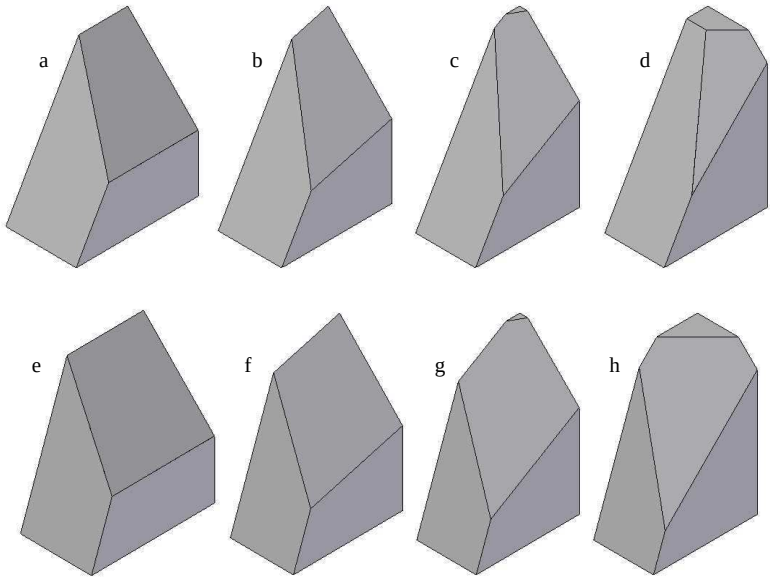

Figure 2.11: Triangular valley test pieces

a) $\theta_w = 60^o$, $\theta_v = 0^o$ b) $\theta_w = 60^o$, $\theta_v = 15^o$ c) $\theta_w = 60^o$, $\theta_v = 30^o$ d) $\theta_w = 60^o$, $\theta_v = 45^o$

e) $\theta_w = 60^o$, $\theta_v = 0^o$ f) $\theta_w = 60^o$, $\theta_v = 15^o$ g) $\theta_w = 60^o$, $\theta_v = 30^o$ h) $\theta_w = 60^o$, $\theta_v = 45^o$

The parabolic valley geometry is varied with changing the variable ‘a’ in the parabolic equation, $y = ax^2 + bx + c$, setting b = 0 and c = 0. The variable ‘a’ is assigned values of 0.04, 0.055 and 0.075. This allowed the characteristic width of the parabola to widen as the variable ‘a’ decreased (as illustrated in figure 2.12). The parabolic valley is cut into the wedge such that the y-axis lies coincident on the wedge edge. The geometry is then rotated along this axis to extrude a paraboloid with axis of symmetry lying coincident on the wedge edge. The three parabolic valleys are illustrated in figure 2.13. All parabolic valleys are manufactured with a 60-degree wedge.

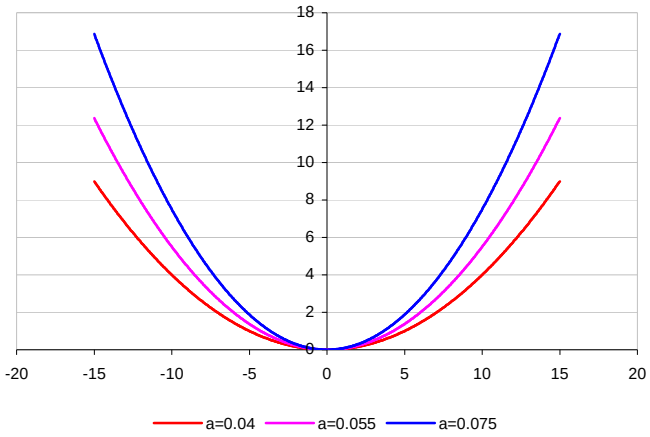

Figure 2.12: Graphical representation of the parabolic valley geometries

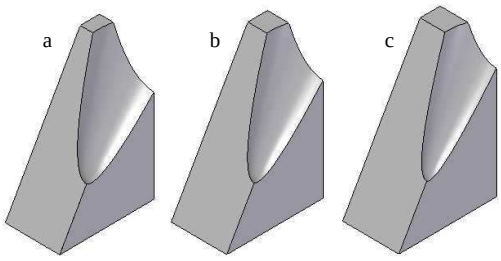

Figure 2.13: Parabolic valley test pieces
a) a = 0.04 b) a = 0.055 c) a = 0.075

The conical valleys have a conical angle of 10 and 20 degrees measured from the axis of symmetry (y axis on figure 2.14), which again is coincident to the wedge edge. The geometry is then rotated along this axis to extrude a cone with axis of symmetry lying coincident on the

wedge edge. The two conical valleys can be seen in figure 2.15. Both conical valleys are manufactured with a wedge of 60-degree inclination.

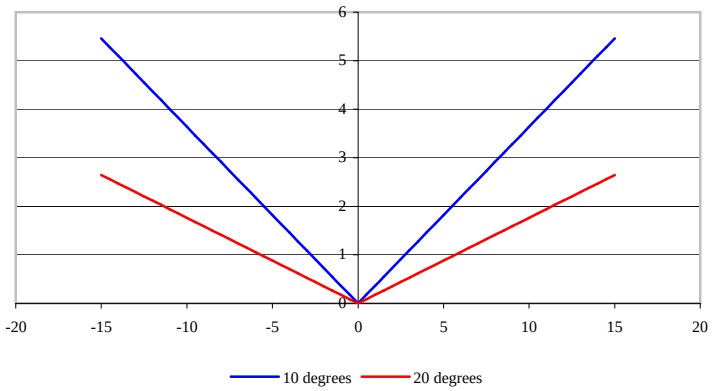

Figure 2.14: Graphical representation of the conical valley geometries

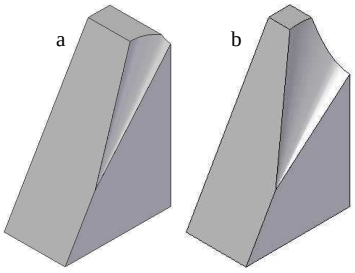

Figure 2.15: Conical valley test pieces
a) 10-degree conical cut out b) 20-degree conical cut out

Both the parabolic and conical valleys were manufactured on a CNC machine due to the complex geometry (Refer to appendix C for details), while the rectangular and triangular could be manufactured using cutting and milling machines. The rectangular valleys have an optical glass insert so that the reflection off the valley floor could be observed. Two optical glass pieces were manufactured to be interchangeable between the eight test pieces. The geometric cut out on the wedges for the glass inserts of the rectangular valleys can be seen in figure 2.16. The glass insert was secured in position using a pressure plug. The glass insert was held in place using silicone, which could be removed when the test piece needed to be changed. The cut out on the rectangular valley wedges could only be accomplished using a CNC machine.

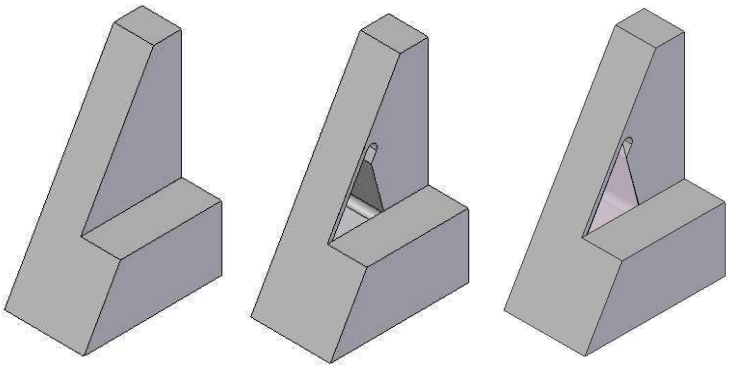

Figure 2.16: Rectangular valley test piece ($\theta_w = 60^o$, $\theta_v = 0^o$) with glass insert

The three hill geometries were designed to be interchangeable. The different hill protrusions were manufactured separately from the 60-degree wedge. The various hill geometries were attached to the wedge by two screws that secured the hill geometry on the wedge surface. Figure 2.17 illustrates the triangular, parabolic and conical hill test pieces.

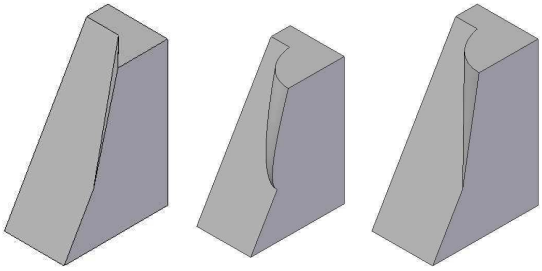

Figure 2.17: Triangular, parabolic and conical hill test pieces